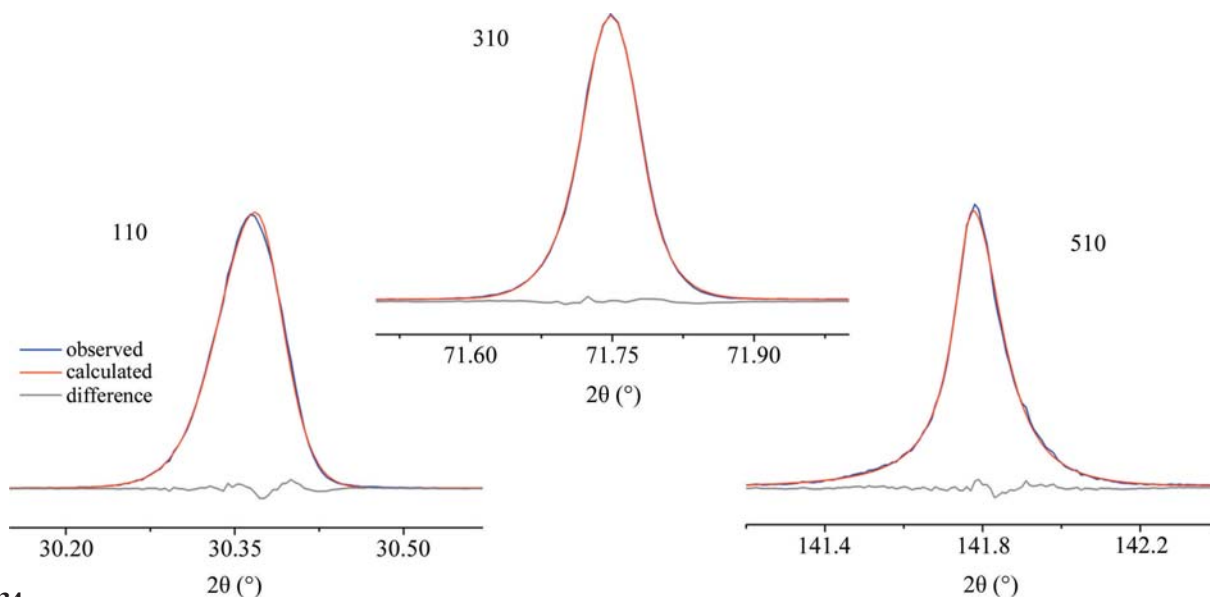
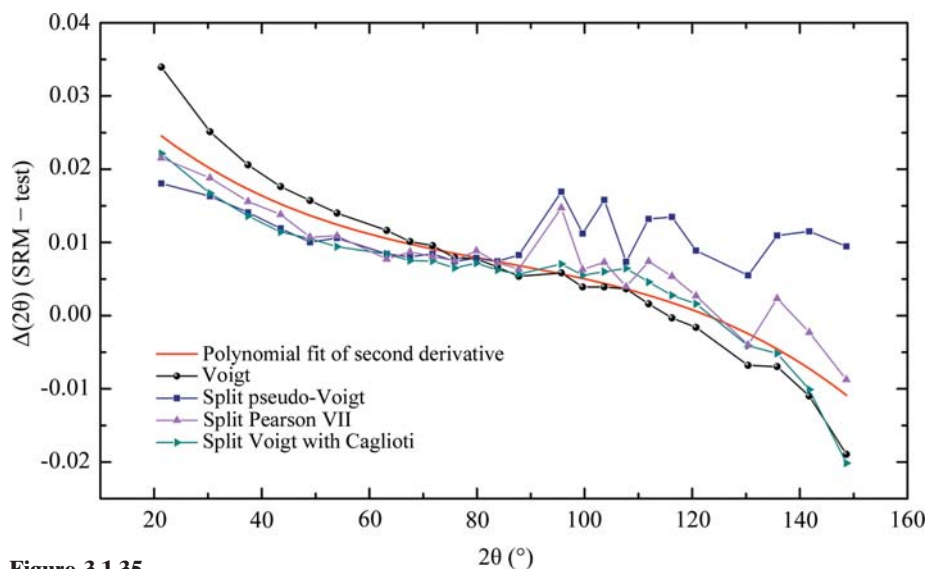


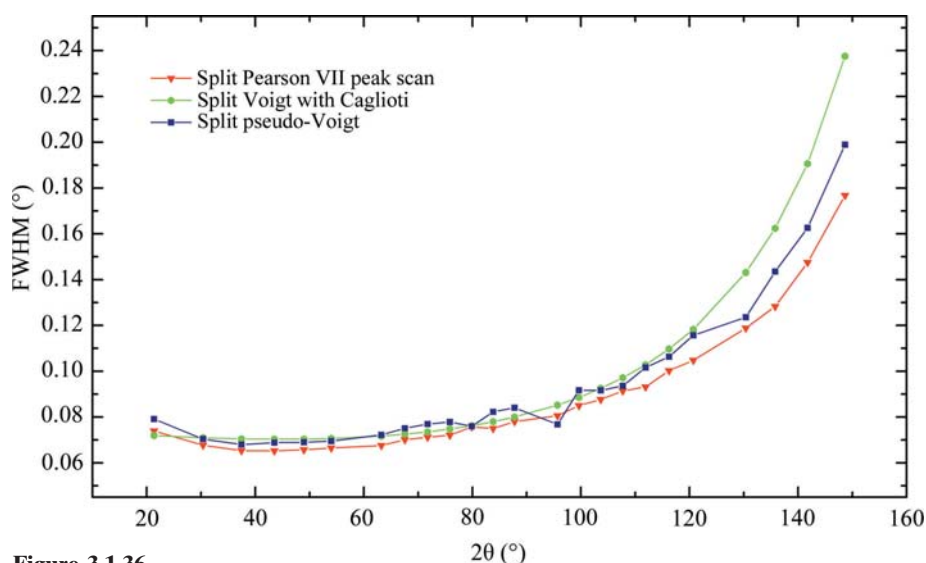
## 3.1. OPTICS AND ALIGNMENT OF THE LABORATORY DIFFRACTOMETER

**Figure 3.1.34**

Fits of a split Pearson VII PSF to data from SRM 660b collected using a Johansson IBM.

**Figure 3.1.35**

$\Delta(2\theta)$  curves from the NIST machine configured with a Johansson IBM, illustrating a comparison of results from second-derivative and various profile-fitting methods. Data are from SRM 660b.

**Figure 3.1.36**

FWHM data from SRM 660b collected using the NIST machine configured with a Johansson IBM, illustrating a comparison of results from various profile-fitting and data-collection methods.

and, to a lesser extent, the split Pearson VII PSFs at high angle. However, the more accurate peak positions are obtained from the more intense reflections, indicating that higher-quality data may improve the results. Improvements in FWHM determination with the use of an IBM are illustrated in Fig. 3.1.36, where it can be seen that the pseudo-Voigt and Pearson VII yield values for the FWHM that differ in a systematic manner, but to a reduced extent than with the conventional data. The virtues of the peak-scan data are illustrated by the continuity of the FWHM values of Fig. 3.1.36 relative to the discontinuities observed in the corresponding data from the conventional scans that were fitted with the pseudo-Voigt PSF. The results from the use of the Caglioti function in Fig. 3.1.36 illustrate that otherwise noisy FWHM data are effectively smoothed out, but a significant bias at high angle is indicated.

FWHM values from the machine equipped with the IBM and PSD are shown Fig. 3.1.37, again with data from SRM 660b. These values were obtained from fits of the split Pearson VII PSF using uniform weighting. The resolution improvement from the use of the PSD is due to the 75  $\mu\text{m}$  strip width, as opposed to the 200  $\mu\text{m}$  receiving slit used with the scintillation detector. This is analogous to a reduction in the width of the top-hat function used to model the impact of the receiving slit or silicon strip width as discussed in Section 3.1.2. The impact is greatest at low  $2\theta$  angles where the other contributions to the overall breadth are small. With increasing  $2\theta$  angle, the contribution of a top-hat function to overall breadth is reduced because it is being convoluted with profiles influenced by ever-increasing spectral dispersion. The improve-